


Research Article

Comparative Experimental Study on Strength Properties of Red Clay Modified by Cement and Industrial Solid Waste Powder

Xianlong Lu ¹, Qiang Yu,¹ Jiayu Xu,² Bing Yue,³ and Mingqiang Sheng ^{1,2}

¹School of Civil and Environmental Engineering, Nanchang Institute of Science and Technology, Nanchang 330108, China

²School of Infrastructure Engineering, Nanchang University, Nanchang 330031, China

³School of Engineering and Technology, China University of Geosciences (Beijing), Beijing 100083, China

Correspondence should be addressed to Xianlong Lu; luxianlong@ncpu.edu.cn

Received 5 August 2023; Revised 20 October 2023; Accepted 20 November 2023; Published 15 December 2023

Academic Editor: Navaratnarajah Sathiparan

Copyright © 2023 Xianlong Lu et al. This is an open access article distributed under the Creative Commons Attribution License, which permits unrestricted use, distribution, and reproduction in any medium, provided the original work is properly cited.

Because of the existence of clay minerals such as montmorillonite in red clay, the strength of red clay decreases significantly as water content increases. This study aims to improve the strength of red clay by using three different kinds of industrial solid waste powder, i.e., steel slag (SS) powder, fly ash (FA), and ground-granulated blast furnace slag (GGBS). At the same time, the ordinary Portland cement (OPC) was selected as a comparison of the improvement effect on the strength of red clay modified by the aforementioned industrial solid waste powder. The properties of the red clay and the industrial solid waste powder were documented comprehensively. The unconfined compressive strength (UCS) tests were conducted on the specimens of the red clay and the red clay modified by the OPC, SS, FA, and GGBS, which had been cured for 3, 7, and 21 days at a temperature of 25°C, respectively. The results showed that the strength of red clay can be significantly improved by the three kinds of industrial solid waste powder. After a 21-day curing period, the experimental results showed that the UCS of the red clay modified by 7% SS, 5% FA, and 5% GGBS increased by 252%, 131%, and 140% compared to that of the red clay without modification. However, the modification effects of the SS, FA, and GGBS on the red clay were generally inferior to that of the OPC. By observing the microstructures of the modified clay, the mechanism of industrial solid waste powder and cement improving the strength of the red clay was analyzed. The findings in this study can provide a reference for improving subgrade strength by a soil-modification method in road constructions.

1. Introduction

Red clay, as a common roadbed filler, is widely distributed in tropical and subtropical regions of southern China [1]. Due to the high content of clay minerals, when red clay absorbs water, the water fills the gaps between the clay particles [2]. This phenomenon leads to a volume expansion of pores in the red clay particles, which in turn results in a decrease in the bonding strength of the clay particles. Therefore, the red clay has high strength when the moisture content is low. However, when the moisture content is increased, the strength of the red clay will rapidly decline [3, 4]. Therefore, the red clay subgrade often faces the problem of differential settlements under loadings during the rainy season.

The existing researches indicate that the addition of cement can greatly enhance the connection between the

clay particles and significantly improve the cohesion of red clay [5]. The copolymer composed of cement and red clay can be used as the subgrade, which can make full use of the in situ red clay while meeting the requirements of engineering construction. However, the production of cement is obviously a process of high energy consumption and carbon emissions. The carbon emissions caused by the production of Portland cement account for about 7% of the global anthropogenic carbon dioxide emissions [6]. China's cement production accounts for 60% of the world's total cement production [7]. Therefore, reducing the indirect carbon emissions caused by using cement has practical significance for achieving China's energy-saving and emission-reduction targets.

At the same time, various kinds of industrial solid wastes have been generated in industrial production, and many of them have not been utilized as resources and have been

directly discarded. For example, steel slag (SS) and blast furnace slag (BFS) are the main solid wastes in the steel industry; for every ton of steel produced in the steel industry, 150–200 kg of SS are generated. Most of the SS is dumped, leading to land resource occupation issues [8]. The annual generation of BFS from the iron–steel metallurgical industry is approximately 150 million metric tons in China. There is a further growth possibility, though the utilization rate of BFS is higher than that of SS [9]. Fly ash (FA) is a byproduct of coal combustion in thermal power plants. More than 160 million tonnes of FA are presently generated annually, and nearly half of them have not been utilized, resulting in serious land occupation and air pollution [10]. In fact, these abandoned industrial wastes have the potential to improve the mechanical properties of soil [11–13]. In the existing research on the modification of red clay, waste tire rubber powder and ground-granulated BFS (GGBS) have been applied and achieved positive results [14, 15]. Using these industrial wastes instead of cement to improve the properties of soils can indirectly reduce a lot of carbon emissions and save a lot of energy. At the same time, it can promote the resource utilization of industrial solid waste, thus to reduce the demand for landfill sites and save land resources [16].

The current research focuses on the modification effect of a single type of solid waste on red clay, and there is a lack of comparative research on the modification effect of different kinds of solid waste. This study aims to provide a reference for practical engineering construction by comparing the influence of different kinds of solid waste materials and cement on the strength of red clay. Therefore, in this study, the three different kinds of industrial solid waste powder, i.e., SS, FA, and GGBS, were selected as additives to improve the strength of red clay, and the ordinary Portland cement (OPC) was also selected as a comparison of the improvement effect. The properties of the red clay and the industrial solid waste additives were all investigated and documented comprehensively. The unconfined compressive strength (UCS) tests were conducted on the specimens of the red clay and the red clay modified by the OPC, SS, FA, and GGBS, respectively. In addition, the scanning electron microscope (SEM) was used to infer and analyze the change mechanism of the UCS of the red clay modified by the OPC, SS, FA, and GGBS, respectively.

2. Materials and Methods

2.1. Properties of the Red Clay. The red clay in this study was collected from Nanchang City, Jiangxi Province, China, which belongs to a typical subtropical monsoon region [17]. The site for red clay excavation was a newly excavated highway slope.

The proctor compaction curve of red clay is shown in Figure 1. It can be determined that the optimal moisture content (OMC) of the red clay is 16.36% with a maximum dry density (MDD) of 1.66 g/cm³.

In order to investigate the natural moisture content of red clay under different climatic conditions, the samples were collected for 14 consecutive days without precipitation and 48 consecutive hours of rainfall, respectively. It was

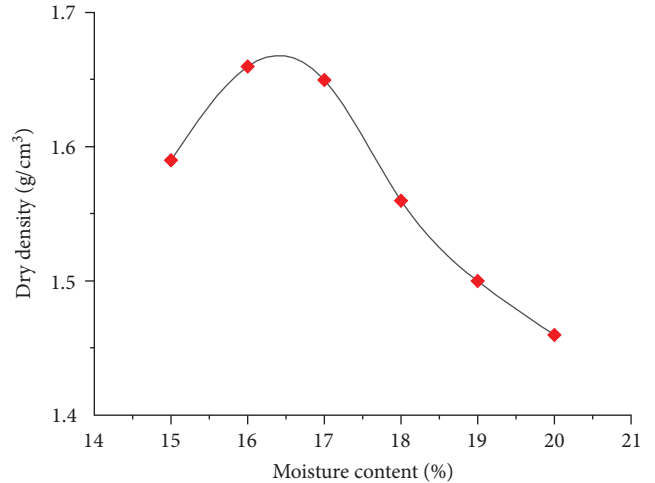


FIGURE 1: Proctor compaction curve of red clay. The red dots represent the specific values obtained from the experiment.

TABLE 1: Atterberg limits test results.

Atterberg limits	Value
Liquid limit, LL (%)	47.70
Plastic limit, PL (%)	18.10
Plasticity index, PI	29.60

indicated that the moisture contents of the red clay were 11.63% and 24.53% under the 14-day-without-rainfall and 48-hr-continuous-rainfall conditions.

In addition, the plasticity characteristics of red clay were determined by the Atterberg limits tests, including liquid limit, plastic limit, and plastic index, as summarized in Table 1.

The particle size distribution of the red clay was tested by a wet laser particle size analyzer, and the particle size distribution curve is shown in Figure 2.

Based on the Casagrande plasticity chart and the Atterberg limits shown in Table 1, the red clay can be categorized as low liquid limit clay according to the Unified Soil Classification System, ASTM D 2487 [18].

The microstructure of the red clay is observed by an SEM (Phenom ProX G6 Desktop SEM, Thermo Fisher Scientific, the United States). Figure 3 shows the SEM images of the red clay with different magnifications.

In addition, the X-ray spectrofluorometer (D8 Advance, Bruker, Germany) was used to conduct the X-ray fluorescence (XRF) test on the red clay, and the test results are shown in Table 2.

2.2. UCS Tests of Red Clay with Different Moisture Contents. Referring to the method of specimen preparation in ASTM 2166 [19], cylindrical specimens with dimensions of 39 mm in diameter and 80 mm in height were prepared using remolded red clay. Figure 4 shows the red remolded clay sample and a completed specimen, respectively.

A strain-controlled unconfined pressure machine was used to test the UCS specimens of the red clay. The UCS of each specimen is determined by Equation (1):

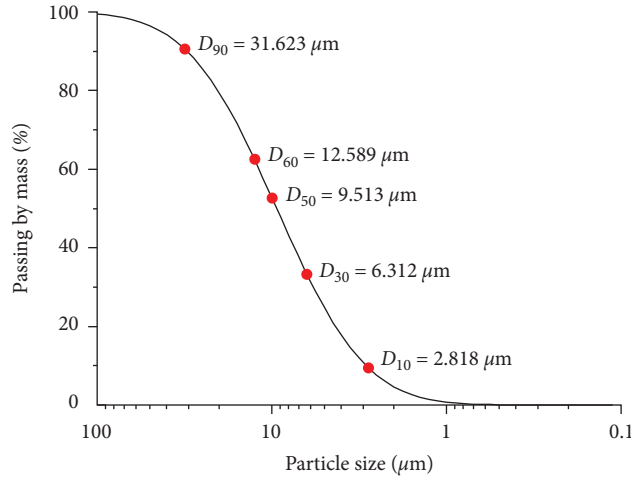


FIGURE 2: Particle size distribution of the red clay. The red dots mark the representative particle size of the soil.

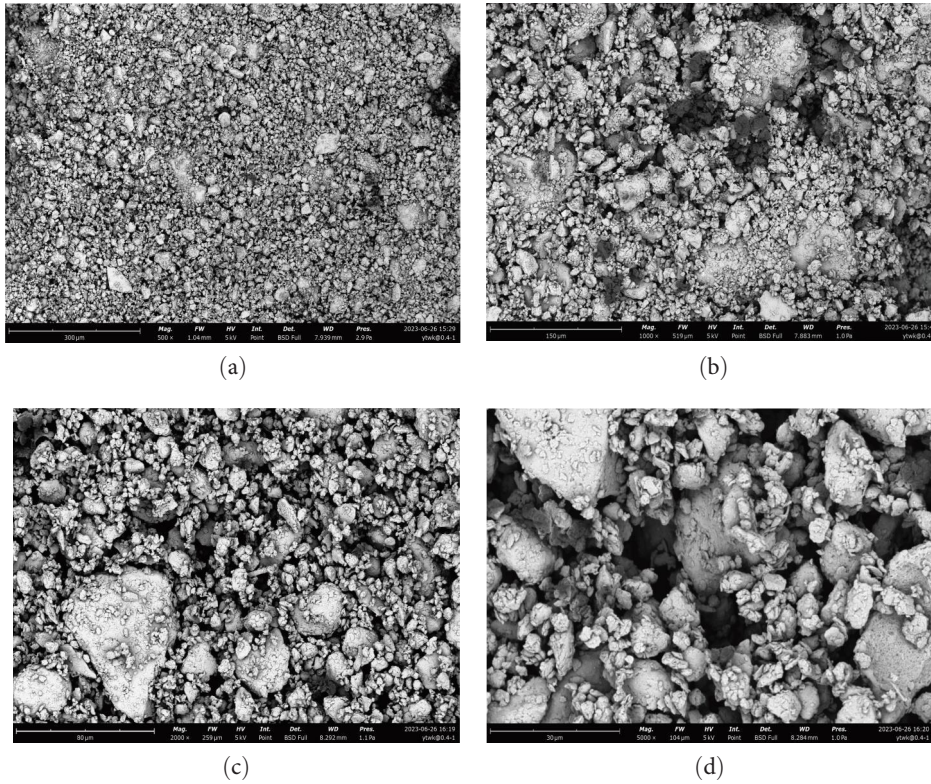


FIGURE 3: SEM images of the red clay: (a) 500x; (b) 1,000x; (c) 2,000x; (d) 5,000x.

$$\sigma = \frac{CR}{A_a} \times 10, \tag{1}$$

where C is the calibration coefficient of the force measuring ring ($N/0.01 \text{ mm}$), R is the force meter reading (0.01 mm) when the maximum axial stress is measured by the unconfined pressure tester (or the axial relative deformation of the sample reaches 15% when there is no obvious maximum axial stress), and A_a is the area of the shear zone (cm^2).

In this study, the UCS test specimens were prepared by the red clay samples with moisture contents of 5%, 10%, 15%, 20%, 25%, and 30%, and the dry density of the samples was controlled at 1.63 g/cm^3 . Three parallel specimens were tested for each moisture content to obtain an average value of the UCS. Table 3 shows the UCS of the red clay at different moisture contents.

As shown in Table 3, the UCS shows a significant decrease as the moisture content of the red clay increases from 5% to 30%. In addition, as the moisture content increases, the failure

TABLE 2: Chemical composition of the red clay and the SS, FA, and GGBS used in this study.

Chemical composition	Content (%)			
	Red clay	FA	SS	GGBS
Calcium oxide (CaO)	0.74	47.40	41.22	59.31
Silicon dioxide (SiO ₂)	52.99	15.82	6.32	16.31
Aluminum oxide (Al ₂ O ₃)	18.78	10.67	2.88	10.24
Ferric oxide (Fe ₂ O ₃)	13.48	4.96	22.44	1.46
Magnesium oxide (MgO)	1.04	4.49	5.68	5.63
Sulfate oxide (SO ₃)	0	—	0.59	—
Sodium oxide (Na ₂ O)	0.07	0.65	0.37	0.43
Potassium oxide (K ₂ O)	5.06	0.96	0.33	0.57
Phosphorus pentoxide (P ₂ O ₅)	0.08	0.06	—	—
Manganese oxide (MnO)	0.17	0.37	3.80	1.00
Zirconia (ZrO ₂)	0.52	0.32	0.14	0.45
Chloride (Cl)	0	1.24	0.06	0.06
Sulfur (S)	0.02	1.78	—	1.22
Strontium oxide (SrO)	0.06	0.67	0.17	0.67
Loss of ignition	4.97	8.20	12.77	—

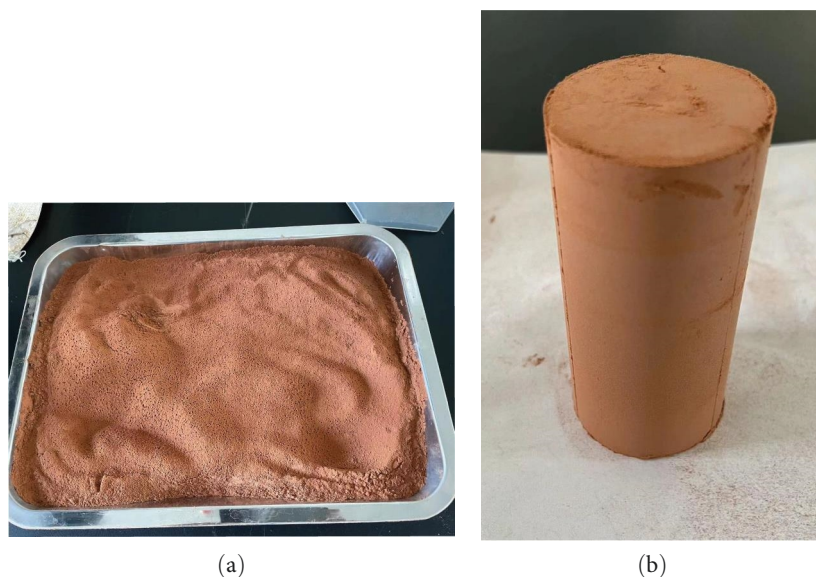


FIGURE 4: The red clay sample and a completed specimen for the UCS test: (a) red clay sample; (b) UCS test specimen.

TABLE 3: The UCS of the red clay with different moisture contents.

Moisture content, w (%)	5	10	15	20	25	30
UCS (kPa)	125.00	104.10	83.28	66.63	62.46	33.13

mode of the specimens tends to be more similar to a plastic failure mode. Figure 5 demonstrates the typical damaged images of the specimens. It can be seen that the failure mode of the red clay specimens transitioned from an obvious shear failure to a plastic deformation with a lateral expansion.

2.3. Composition and Form of Additives. The OPC is widely used in China. Therefore, in this study, the OPC of P.O42.5 was selected which was produced by the China

United Cement Group. The SS was chosen from a steel plant in Shijiazhuang City, Hebei Province, China. The C-class FA was chosen which was produced by a thermal power plant in Gongyi County, Henan Province, China, and the fuel was brown coal. The GGBS was collected from a BFS powder processing plant in Xinxiang City, Henan Province, China. Figure 6 shows the samples of the OPC and the other three kinds of industrial solid waste powder in this study.

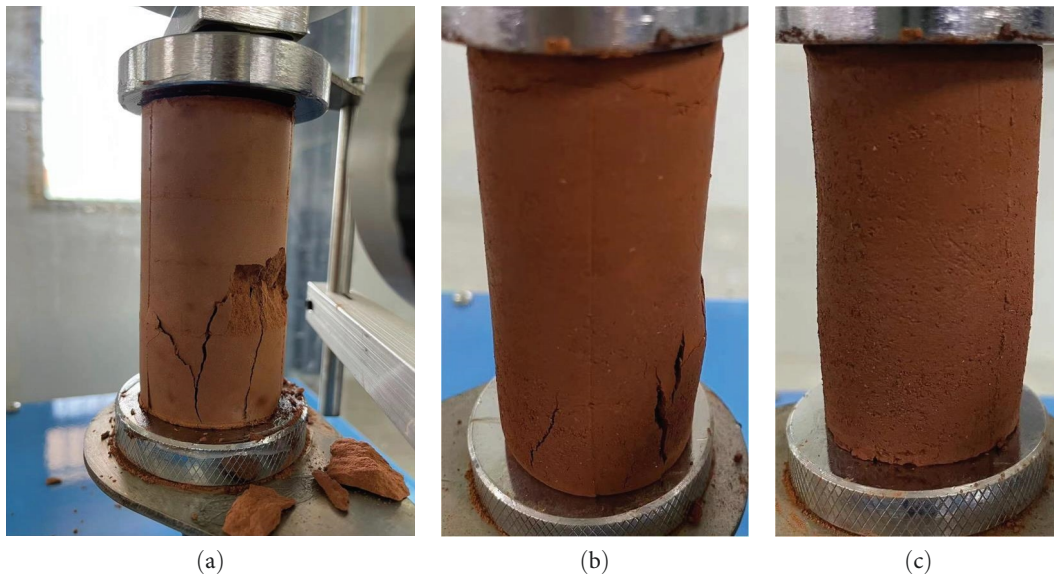


FIGURE 5: The UCS test failure of the red clay specimens with different moisture contents: (a) 5%; (b) 15%; (c) 25%.

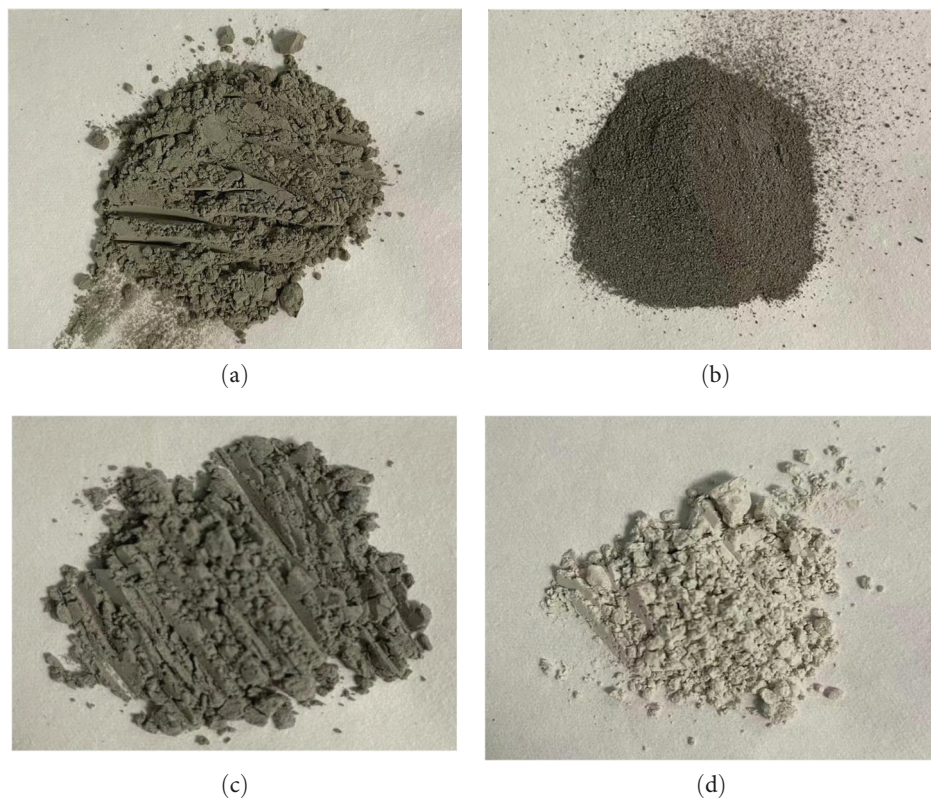


FIGURE 6: Additive samples used in this study: (a) OPC; (b) SS; (c) FA; (d) GGBS.

Particle size analysis was also carried out for the three kinds of industrial solid waste powder of SS, FA, and GGBS, as shown in Figure 7. Overall, the particle size in a decreasing sequence of the three kinds of solid waste powder was SS, FA, and GGBS.

Figure 8 shows the scanning electron photomicrograph of the SS, FA, GGBS, and OPC structures, respectively. In

addition, the XRF was also carried out on the SS, FA, and GGBS, as summarized in Table 2.

2.4. Preparation for the UCS Tests of Red Clay Modified by OPC, SS, FA, and GGBS. Based on the aforementioned Atterberg limits and the proctor compaction test results of red clay, the red clay with a moisture content of 15% was

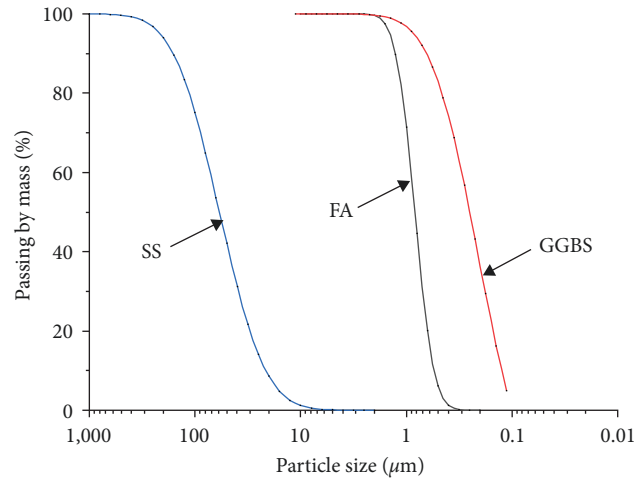


FIGURE 7: Particle size distribution cures of the SS, FA, and GGBS in this study.

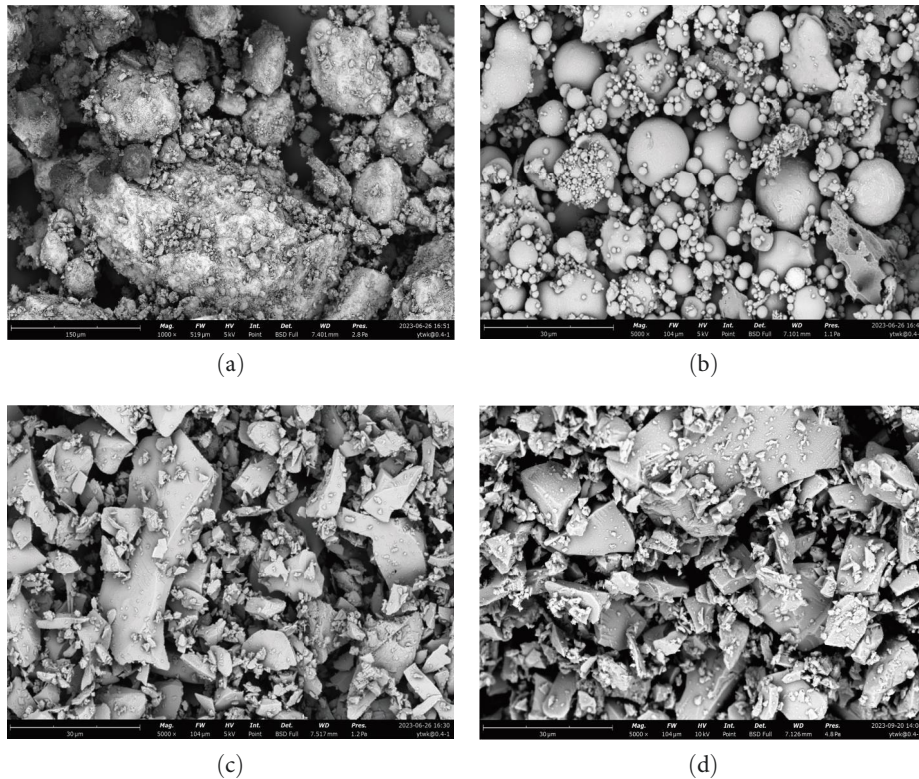


FIGURE 8: SEM images of the industrial solid waste powders in this study: (a) SS; (b) FA; (c) GGBS; (d) OPC.

determined for the preparation on the UCS test specimens, which would be modified by the OPC, SS, FA, and GGBS, respectively. The reason for selecting a moisture content of 15% of the red clay was mainly based on the following considerations:

First, according to the compaction test, the OMC of the red clay was 16.3%. As a result, the 15% moisture content can almost satisfy the compaction requirements of the red clay in engineering constructions. Second, considering the climatic condition of the region where the red clay is located in this

study, the 15% moisture content is very closer to and slightly higher than the natural moisture content of the red clay in most periods. Therefore, the selection of this moisture content may be more convenient for the application of research results in actual engineering in the region. Third, the 15% moisture content did not reach the plastic limit of the red clay, which would be more conducive to a uniform mixing of soil-additive mixtures.

The specific following procedures were used to obtain red clay samples with 15% moisture content: drying and

TABLE 4: Weight and additive content of specimens for the UCS tests in different groups.

Additive type	Group number	Dry mass proportion of additive (%)	Additive content (g)	Weight of mixed specimens (g)
OPC	1	1	1.57	158.14
	2	3	4.70	161.27
	3	5	7.83	164.40
	4	7	10.96	167.53
	5	9	14.09	170.66
SS	6	1	1.57	158.14
	7	3	4.70	161.27
	8	5	7.83	164.40
	9	7	10.96	167.53
	10	9	14.09	170.66
FA	11	1	1.57	158.14
	12	3	4.70	161.27
	13	5	7.83	164.40
	14	7	10.96	167.53
	15	9	14.09	170.66
GGBS	16	1	1.57	158.14
	17	3	4.70	161.27
	18	5	7.83	164.40
	19	7	10.96	167.53
	20	9	14.09	170.66

crushing the red clay, evenly adding water to the dried red clay using a spray can until the red clay moisture content reaches 15%, sealing the red clay, and finally maintaining the red clay sample for more than 12 hr. During the process of adding water and mixing, the red clay particles may form small pieces due to cohesions. Therefore, sealing and maintaining the red clay samples for more than 12 hr would make the water evenly distributed within the red clay pieces.

After 12 hr for sealing, the additives were added into the aforementioned red clay samples and mixed evenly. In this study, each additive of the OPC, SS, FA, and GGBS was added in a proportion of 1%, 3%, 5%, 7%, and 9% of the dry mass of the red clay, respectively, as shown in Table 4. Each group of the specimens was sealed and cured for 3, 7, and 21 days at a temperature of 25°C. In addition, three parallel specimens of each group with the same kind of additive, the same dosage of additive, and the same curing age were chosen. The average value of these three parallel specimens was determined as the UCS for the group. As a result, a total of 180 specimens were prepared for the UCS tests in this study.

Similar to the UCS tests of red clay, cylindrical specimens with dimensions of 39 mm in diameter and 80 mm in height were prepared by the red clay modified by the OPC, SS, FA, and GGBS, respectively, and the dry mass of the modified red clay was controlled at a density of 1.63 g/cm³.

It should be noted that referring to the method suggested by Khoury et al. [20], the moisture content of all the UCS test specimens was increased to 25% after the curing periods of 3, 7, and 21 days, respectively. Therefore, the UCS test specimens for the red clay modified by the OPC, SS, FA, and GGBS were at a moisture content of 25%. Figure 9 shows

the device for increasing the moisture content of the UCS test specimen in this study.

Overall, the sample preparation method used in the study not only could be conducive to the sufficient mixing of the additives and red clay but also could facilitate the investigation of the improvement in the strength of the red clay modified by the additives after a change of the moisture content due to precipitations.

3. Results and Discussion

3.1. Proctor Compaction Tests of Soil-Additive Mixtures. Figure 10 shows the proctor compaction test results conducted on the red clay modified by the OPC, SS, FA, and GGBS with a proportion of 9%. As indicated in Figure 10, the OMC of the soil-additive mixtures with SS, FA, GGBS, and OPC was 16.82%, 16.55%, 16.80%, and 17.65%, with a corresponding MDD of 1.77, 1.65, 1.68, and 1.76 g/cm³, respectively.

From the results of the proctor compaction tests, as shown in Figure 10, it can be seen that the addition of OPC and SS has a more significant effect on improving the MDD of the soil-additive admixture, and OPC can improve the OMC of the soil-additive admixture, which would reduce the plasticity of the red clay modified by the OPC.

3.2. UCS of the Modified Red Clay. Figure 11 shows the comparisons of the variations of UCS against the added proportion of the additives when the red clay was modified by OPC, SS, FA, and GGBS after the curing period of 3, 7, and 21 days, respectively. For ease in comparison, the UCS of the red clay without modification at a moisture content of 25% is also marked in Figure 11.

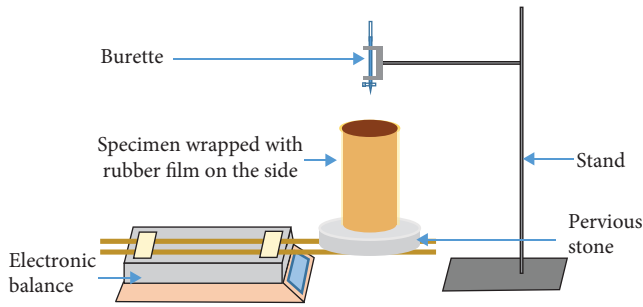


FIGURE 9: The sketch of devices for increasing the moisture content of the specimen.

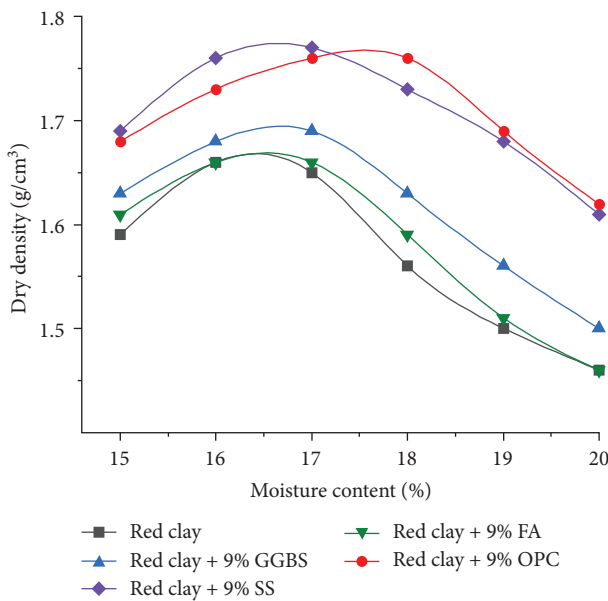


FIGURE 10: Proctor compaction curves of the soil-additive mixtures.

It can be seen that the UCS of the red clay modified by OPC and the other three kinds of industrial solid wastes showed a significant improvement in the UCS compared to that of the red clay without modification. However, the relationship between UCS and the added proportion of the additives of OPC, SS, FA, and GGBS display different trends.

First, when the OPC content ranges from 1% to 5%, the UCS of the modified red clay is significantly improved, as shown in Figure 11(a). However, as the OPC content reaches 5%, increasing the OPC content can no longer significantly increase the UCS of the modified red clay. The effect of curing time on the OPC of the modified red clay can be described as follows: the strength of the modified red clay cured for 7 and 21 days is very similar, slightly higher than that of specimens cured for 3 days. After a 7-day curing, the UCS of the red clay modified by 5% OPC addition is 267.1 kPa, which is increased by 328% compared to the red clay without modification.

Second, for the red clay modified by the SS, the UCS shows an overall trend of increasing as the SS dosage ranges from 1% to 7%, as shown in Figure 11(b). However, when the SS dosage is 9%, the UCS decreases compared to that of the

red clay modified by the SS at a dosage of 7%. Therefore, the maximum UCS is 220.0 kPa, which occurred under the 7% SS dosage with a 21-day curing condition. Compared to the red clay without additives, the UCS of the red clay modified by the SS increases by 252%.

Third, for the red clay modified by the FA, the UCS generally indicates a slow-increasing trend as the FA content ranges from 1% to 5% and reaches a maximum of 121.1 kPa with an increase by 131% compared to the red clay without modification, as shown in Figure 11(c). However, when the FA content ranges from 5% to 9%, the strength of the modified red clay shows a slow decreasing trend as increasing the FA content, and the variation of the UCS of the modified clay caused by the change of the FA content is relatively small. In general, with the extension of the curing period, there is no significant change in the UCS of the modified red clay.

Forth, for the red clay modified by the GGBS, the UCS also shows a trend of first increasing and then decreasing as the GGBS content increases, as shown in Figure 11(d). In general, with the increase in curing time, the UCS increased slightly. The UCS can obtain a maximum of 123 kPa, which occurred under the 5% GGBS dosage with a 21-day curing condition, with an increase by 140% compared to the red clay without additives.

Overall, the modification effect of the OPC was better than that of the other three kinds of solid wastes. When the OPC was used as an additive, it had a significant effect in a short period of time. However, after the OPC content reached 5%, increasing the OPC content could no longer significantly improve the UCS of the modified red clay. The modification effect of the SS was generally better than those of the FA and the GGBS. The specimens with 7% SS content and 21 days curing reached 82% of those with 5% OPC content and 7 days curing period. The curing time has a more significant improvement on the UCS of the SS-modified specimens. Under the condition of 5% additive content and 7 days of curing, the UCS of specimens modified by FA increased by more than twice, and the degree of improvement in UCS of specimens modified by GGBS was also similar.

3.3. Failure Mode of the Modified Red Clay. Figure 12 shows the typical failure modes of the red clay modified by the OPC, SS, FA, and GGBS after the unconfined compression tests, respectively. By observing the morphology of the specimens after failure, compared with the failure mode in the previous clay modification experiments [20, 21], the failure mode of the red clay modified by the OPC was a single-slope shear failure, but that of the red clay modified by the SS was tension failure. However, the failure modes of the red clay modified by the FA and GGBS exhibited the characteristics of diagonal cracks and bulging failures, respectively.

3.4. Micromorphology of Different Additives Modified Red Clay. The change mechanism of the UCS can be inferred by observing the SEM images and by comparing the microstructures of the red clay after and before modification. Therefore, in this study, SEM was used to observe the

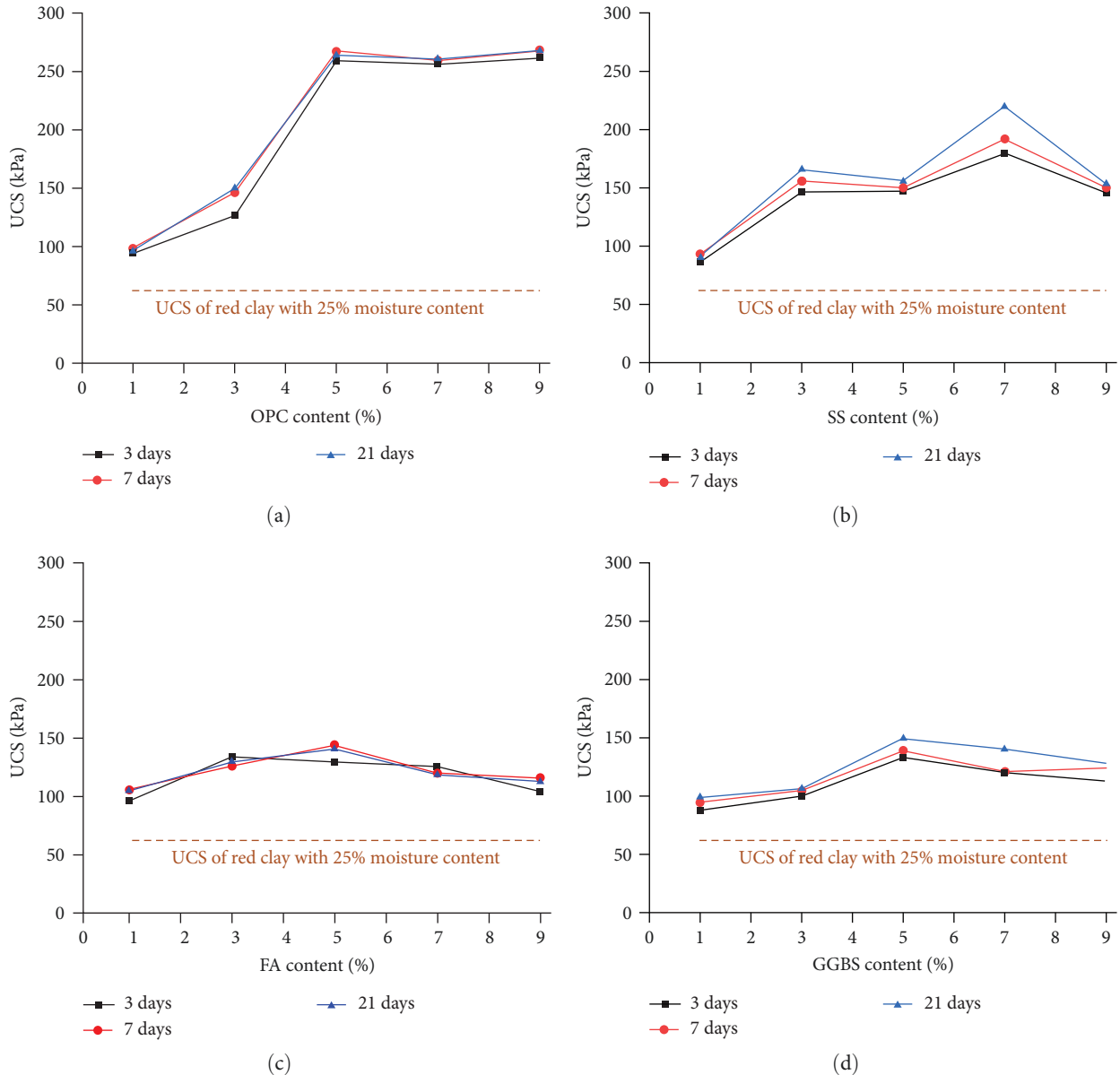


FIGURE 11: Comparison of the variations of UCS against the content of different additives: (a) OPC; (b) SS; (c) FA; (d) GGBS.

specimen with the highest UCS of the red clay modified by the OPC, SS, FA, and GGBS, respectively, as shown in Figure 13.

It can be seen from the SEM image of the red clay modified by the OPC, granular hydrate calcium silicate (CSH) and plate-like CH can be observed. The red clay particles are bonded with these hydration products, and the gaps between the red clay particles are also filled with these hydration products, as indicated by Figure 13(a). A similar phenomenon in Figure 13(b) can also be observed in the SEM image of the red clay modified by the SS. The existence of CSH gel makes the dispersed clay particles bond into a whole, thus to improve the strength of the clay. This phenomenon mainly occurs around the SS particles. As shown in Figure 13(c), the SEM image of the red clay modified by the FA shows that the shape of red clay particles has almost not changed, indicating

that almost no hydration product is produced. In addition, as shown in Figure 13(d), the SEM image of the red clay modified the GGBS; it can be seen that a portion of GGBS particles are adsorbed on the surface of red clay particles in a surface-to-surface form, and just a small amount of silicates and aluminates can be observed in the gaps between GGBS and red clay particles.

3.5. Discussion on the Modification Mechanism of Different Kinds of Additives. When inorganic materials (OPC and the three kinds of solid wastes of SS, FA, and GGBS in this study) are used as soil modification additives, their effects can be mainly divided into two aspects: the cementation caused by pozzolanic reaction and the improvement in the mechanical properties caused by changes in particle size distribution and density of soil-additive admixture [22]. The OPC, SS, FA,

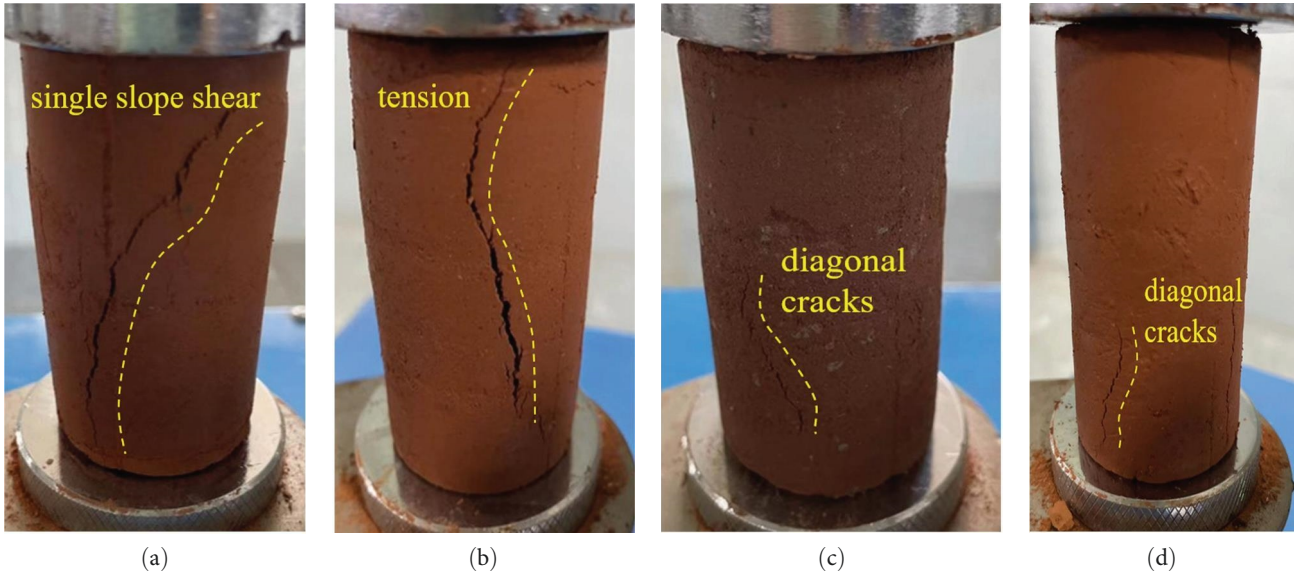


FIGURE 12: Failure modes of the red clay modified by the different additives: (a) OPC; (b) SS; (c) FA; (d) GGBS.

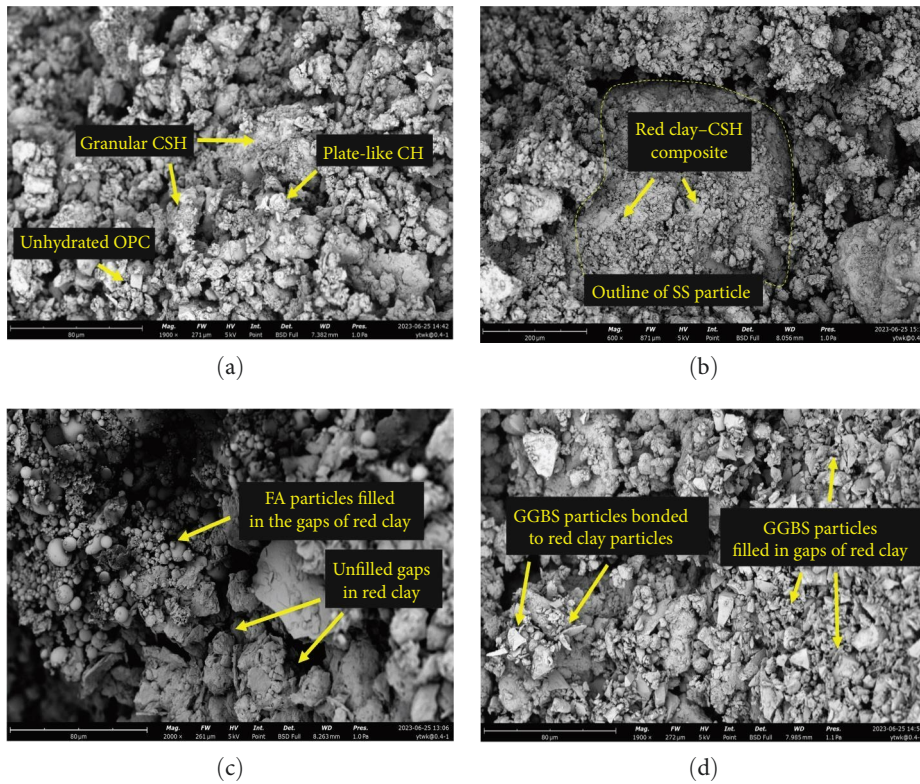


FIGURE 13: SEM images of the red clay modified by different additives: (a) OPC; (b) SS; (c) FA; (d) GGBS.

and GGBS all have potential pozzolanic activities, but the rate of pozzolanic reaction in the OPC was faster than those of the other three kinds of solid wastes [23]. Among the three kinds of solid wastes of SS, FA, and GGBS in this study, the pozzolanic activity of the SS was higher than that of FA and GGBS.

Due to the bonding and filling effects of hydration products, the UCS of the red clay modified by the OPC can be

improved [24]. However, some unhydrated OPC clinker can also be observed. It was obvious that a portion of the water contained in the red clay was not free water but was adsorbed on the clay particles in the form of bound water [25]. Therefore, only a portion of the water in the red clay would participate in the hydration reaction of the OPC, which resulted in insufficient free water for the hydration reaction when the OPC content reached a certain level. Without the generation

of much more hydration products, the strength of the red clay modified by OPC could not be further improved. Due to the high strength of the hardened hydration products, the specimens modified by the OPC had a good rigidity and exhibited a single slope shear failure mode.

The pozzolanic reaction also existed in the red clay modified by the SS, but the hydration products were significantly fewer compared to those of the red clay modified by the OPC. Due to the lack of silicon and aluminum in the SS, the hydration reaction required silicon and aluminum in the red clay. Therefore, the hydration products were mainly generated at the contact surfaces between the SS particles and the red clay particles. When the content of the SS was large enough, it would cause mutual contact between the SS particles, and the contact surface between the SS particles lack bonding, leading to a decrease in the strength of the modified red clay. At the same time, the SS particles were larger than the red clay particles. When the SS particles were dispersed in the red clay, they could play a role in blocking the formation of the shear surface [26], so that the specimens modified by the SS appeared in a tensile failure mode after compression.

For the FA and GGBS, they exhibited a relatively poor pozzolanic activity. Due to FA was generated and collected in high-temperature environments, the FA particles had a large amount of glass phase on the surfaces. Because of the presence of the glass phase, the calcium in the FA was difficult to dissolve in a nonalkaline environment, which resulted in the generation of calcium silicates and aluminum silicates [27]. Therefore, the improvement of the UCS of the red clay modified by the FA was mainly due to the filling effect. While the addition of the FA reached a certain amount, the filling effect was no longer obvious. Because the FA particles appear spherical, it may actually cause a decrease in the overall internal friction force of the modified red clay, thus leading to a decrease in strength. The factors that affected the hydration reaction of GGBS included the chemical composition, specific surface area, the alkali concentration, and the temperature of the environment. Some experimental results have also shown that the initial reaction of the GGBS during hydration produced a porous crystallized hydrated layer of coating of alumino-silicate products on the surface of GGBS particles within a short time of exposure to water [28]. The presence of these coating surfaces hindered further hydration of the internal components of the GGBS particles [29]. Therefore, there were a large number of unhydrated particles in the red clay modified by the GGBS. As a result, the UCS could not be further improved as the GGBS content reached 5%. In general, for the red clay modified by the FA and GGBS, the failure mode was closer to plastic deformation and exhibited bulging failure during compression.

4. Conclusions

The following conclusions can be drawn based on the comparative experimental study on the strength properties of red clay modified by the OPC, SS, FA, and GGBS:

Overall, OPC, SS, FA, and GGBS can all improve the UCS of the red clay to a certain extent. In general, the red

clay modified by the OPC can obtain the largest UCS due to the fastest generation of hydration products. Interestingly, the modification effect of the SS was the best among the other three kinds of solid wastes.

When OPC was used as an additive for red clay modification, it generated more hydration products compared to industrial solid wastes, which can provide more bonding between red clay particles and improve the strength of the modified red clay. However, blindly increasing the OPC content could not continuously improve the strength of red clay modified by OPC, because a large portion of the water in the red clay can not be utilized by the hydration reaction, which hindered the generation of more hydration products.

When SS was used as an additive for modifying red clay, the effect was the best among the three kinds of industrial solid wastes. The modification mechanism of SS was mainly reflected in the following two aspects: first, the red clay particles were bound together by the hydration products produced by SS; second, the larger SS particles hindered the formation of the shear surface.

The modification effects of the FA and GGBS were similar. Similar modification mechanisms exhibited similar effects; the maximum UCS of these two kinds of additive-modified specimens occurred under the condition of 5% dosage, with similar degrees of improvement in the UCS. Neither of the two kinds of additive showed an obvious hydration reaction. The reasons for the lack of hydration reaction in red clay modified by FA and GGBS were that both kinds of solid wastes could not fully exert their pozzolanic activity when added separately.

Data Availability

The datasets used and/or analyzed during the current study are available from the corresponding author upon reasonable request.

Conflicts of Interest

The authors declare that they have no conflicts of interest.

Acknowledgments

The authors would like to acknowledge the supports from the Jiangxi Provincial Department of Education (no. GJJ151242) and from the Graduate Innovation Fund Project of China University of Geosciences, Beijing (no. ZD2023YC032).

References

- [1] J. B. Yuan, Y. He, and J. H. Liu, "Construction of weak expansive red clay on Dongxin expressway in Hunan Province, China," *Journal of Performance of Constructed Facilities*, vol. 30, no. 1, Article ID C4015001, 2016.
- [2] A. Sridharan and M. S. Jayadeva, "Double-layer theory and compressibility of clays," *Géotechnique*, vol. 32, no. 2, pp. 133–144, 1982.
- [3] Y. R. Hu, S. R. Sun, and K. Li, "Study on influence of moisture content on strength and brittle-plastic failure characteristics of

- Xiashu loess,” *Advances in Civil Engineering*, vol. 2023, Article ID 5919325, 10 pages, 2023.
- [4] J. P. Malizia and A. Shakoor, “Effect of water content and density on strength and deformation behavior of clay soils,” *Engineering Geology*, vol. 244, pp. 125–131, 2018.
- [5] B. Yue, Z. Zhao, and Z. Qian, “Influence of five additives on no loading swelling potential of red clay,” *Applied Sciences-Basel*, vol. 12, no. 7, Article ID 3455, 2022.
- [6] L. McDonald, F. P. Glasser, and M. S. Imbabi, “A new, carbon-negative precipitated calcium carbonate admixture (PCC-A) for low carbon portland cements,” *Materials*, vol. 12, Article ID 554, 2019.
- [7] W. Shen, Y. Liu, B. Yan et al., “Cement industry of China: driving force, environment impact and sustainable development,” *Renewable and Sustainable Energy Reviews*, vol. 75, pp. 618–628, 2017.
- [8] S. Chand, B. Paul, and M. Kumar, “Sustainable approaches for LD slag waste management in steel industries: a review,” *Metallurgist*, vol. 60, no. 1-2, pp. 116–128, 2016.
- [9] Y. Li, Y. Liu, X. Gong et al., “Environmental impact analysis of blast furnace slag applied to ordinary portland cement production,” *Journal of Cleaner Production*, vol. 120, pp. 221–230, 2016.
- [10] Z. T. Yao, X. S. Ji, P. K. Sarker et al., “A comprehensive review on the applications of coal fly ash,” *Earth-Science Reviews*, vol. 141, pp. 105–121, 2015.
- [11] J. James and P. K. Pandian, “Industrial wastes as auxiliary additives to cement/lime stabilization of soils,” *Advances in Civil Engineering*, vol. 2016, Article ID 1267391, 17 pages, 2016.
- [12] J. Zheng and W. Qin, “Performance characteristics of soil–cement from industry waste binder,” *Journal of Materials in Civil Engineering*, vol. 15, no. 6, pp. 616–618, 2003.
- [13] N. P. Vignesh, K. Mahendran, and N. Arunachalam, “Effects of industrial and agricultural wastes on mud blocks using geopolymer,” *Advances in Civil Engineering*, vol. 2020, Article ID 1054176, 9 pages, 2020.
- [14] M. Gao, X. Jin, T. Zhao, H. Li, and L. Zhou, “Study on the strength mechanism of red clay improved by waste tire rubber powder,” *Case Studies in Construction Materials*, vol. 17, Article ID e01416, 2022.
- [15] A. Shivaramaiah, A. U. Ravi Shankar, A. Singh, and K. H. Pammar, “Utilization of lateritic soil stabilized with alkali solution and ground granulated blast furnace slag as a base course in flexible pavement construction,” *International Journal of Pavement Research and Technology*, vol. 13, no. 5, pp. 478–488, 2020.
- [16] R. Siddique, “Utilization of waste materials and by-products in producing controlled low-strength materials,” *Resources, Conservation and Recycling*, vol. 54, no. 1, pp. 1–8, 2009.
- [17] M. J. Zhan, L. J. Xia, L. F. Zhan, and Y. H. Wang, “Recognition of changes in air and soil temperatures at a station typical of China’s subtropical monsoon region (1961–2018),” *Advances in Meteorology*, vol. 2019, Article ID 6927045, 9 pages, 2019.
- [18] ASTM International, “Standard practice for classification of soils for engineering purposes (unified soil classification system),” in *ASTM D2487-17, American Society for Testing and Materials*, ASTM International, West Conshohocken, PA, USA, 2017.
- [19] ASTM International, “Standard test method for unconfined compressive strength of cohesive soil,” in *ASTM 2166-16, American Society for Testing and Materials*, ASTM International, West Conshohocken, PA, USA, 2016.
- [20] N. Houry, R. Brooks, S. Y. Boeni, and D. Yada, “Variation of resilient modulus, strength, and modulus of elasticity of stabilized soils with postcompaction moisture contents,” *Journal of Materials in Civil Engineering*, vol. 25, no. 2, pp. 160–166, 2013.
- [21] A. Eslami and D. Akbarimehr, “Failure analysis of clay soil–rubber waste mixture as a sustainable construction material,” *Construction and Building Materials*, vol. 310, Article ID 125274, 2021.
- [22] H. Shoghi, M. Ghazavi, and N. Ganjian, “The effects of chemical admixtures and physical factors on the treatment of dispersive soils,” *Arabian Journal of Geosciences*, vol. 10, Article ID 486, 2017.
- [23] S. Inazumi, S. Intui, A. Jotisankasa, S. Chaiprakaikeow, and T. Shinsaka, “Applicability of mixed solidification material based on inorganic waste as soil stabilizer,” *Case Studies in Construction Materials*, vol. 10, Article ID e00305, 2020.
- [24] Y. Yi, X. Zheng, S. Liu, and A. Al-Tabbaa, “Comparison of reactive magnesia- and carbide slag-activated ground granulated blast furnace slag and portland cement for stabilisation of a natural soil,” *Applied Clay Science*, vol. 111, pp. 21–26, 2015.
- [25] L. Liu, A. Zhou, Y. Deng, Y. Cui, Z. Yu, and C. Yu, “Strength performance of cement/slag-based stabilized soft clays,” *Construction and Building Materials*, vol. 211, pp. 909–918, 2019.
- [26] M. Xu, L. Liu, Y. Deng, A. Zhou, S. Gu, and J. Ding, “Influence of sand incorporation on unconfined compression strength of cement-based stabilized soft clay,” *Soils and Foundations*, vol. 61, no. 4, pp. 1132–1141, 2021.
- [27] J. L. Provis, P. Duxson, R. M. Harrex, C.-Z. Yong, and J. S. J. van Deventer, “Valorisation of fly ashes by geopolymerisation,” *Global Nest Journal*, vol. 11, no. 2, pp. 147–154, 2009.
- [28] R. M. Nidzam and J. M. Kinuthia, “Sustainable soil stabilisation with blastfurnace slag—a review,” *Proceedings of the Institution of Civil Engineers—Construction Materials*, vol. 163, no. 3, pp. 157–165, 2010.
- [29] I. G. Richardson, A. R. Brough, G. W. Groves, and C. M. Dobson, “The characterization of hardened alkali-activated blast furnace slag pastes and nature of the calcium hydrate (C-S-H) phase,” *Cement and Concrete Research*, vol. 24, no. 5, pp. 813–829, 1994.